Polarforschung 84 (1), 23–38, 2014

The Ross-Orogenic Tiger Gabbro Complex (Northern Victoria Land, Antarctica): Insights into the Lower Crust of a Cambrian Island Arc

by Friedhelm Henjes-Kunst[1], Jürgen Koepke[2], Andreas Läufer[1], Solveig Estrada[1], Glen Phillips[3,4], Karsten Piepjohn[1], and Dominique Kosanke[2]

Abstract: Subduction related mafic/ultramafic complexes marking the suture between the Wilson Terrane and the Bowers Terrane in northern Victoria Land (Antarctica) are well-suited for evaluating the magmatic and structural evolution at the Palaeo-Pacific continental margin of Gondwana. One of these intrusions is the "Tiger Gabbro Complex" (TGC), which is located at the southern end of the island-arc type Bowers Terrane. The TGC is an early Palaeozoic island-arc related layered igneous complex characterized by extraordinarly fresh sequences of ultramafic, mafic and evolved lithologies and extensive development of high-temperature high-strain zones. The goal of the present study is to establish the kinematic, petrogenetic and temporal development of the TGC in order to evaluate the magmatic and structural evolution of the deep crustal roots of this Cambrian-aged island-arc. Fieldwork during GANOVEX X was carried out to provide insight into: (i) the spatial relations between the different igneous lithologies of the TGC, (ii) the nature of the contact between the TGC and Bowers Terrane, and (iii) the high-temperature shear zones exposed in parts of the TGC. Here, we report the results of detailed field and petrological observations combined with new geochronological data. Based on these new data, we tentatively propose a petrogenetic-kinematic model for the TGC, which involves a two-phase evolution during the Ross orogeny. These phases can be summarized as: (i) an early phase (maximum age c. 530 Ma) involving tectono-magmatic processes that were active at the deep crustal level represented by the TGC within the Bowers island arc and within a general NE–SW directed contractional regime and (ii) a late phase (maximum age c. 490 Ma) attributed to the late Ross orogenic intrusion of the TGC into the higher-crustal metasedimentary country rocks of the Bowers Terrane under NE–SW directed horizontal maximum stress and subsequent cooling.

Zusammenfassung: Subduktionsgebundene mafisch-ultramafische Komplexe markieren die Sutur zwischen dem Wilson Terrane und dem Bowers Terrane im nördlichen Victoria Land (Antarktis). Diese sind gut geeignet, um die magmatische und strukturelle Entwicklung am paläopazifischen Kontinentrand Gondwanas im Kambrium zu rekonstruieren. Eine dieser Intrusionen stellt der „Tiger Gabbro Complex" (TGC) am südlichen Ende des Inselbogenkomplexes des Bowers Terranes dar. Der TGC ist ein frühpaläozoischer geschichteter Magmatitkomplex mit Inselbogenaffinität, der durch außerordentlich frische Gesteinsabfolgen ultramafischer, mafischer und stärker differenzierter Lithologien und durch hoch-temperierte Scherzonen gekennzeichnet ist. Das Ziel dieser Arbeit ist die Klärung der kinematischen, petrogenetischen und zeitlichen Entwicklung des TGC, um so die magmatische und strukturelle Entwicklung der tief-krustalen Bereiche dieses kambrischen Inselbogenkomplexes zu rekonstruieren. Die Geländeaufnahmen während GANOVEX X wurden mit den Zielen durchgeführt, 1.) die räumlichen Zusammenhänge der verschiedenen Lithologien innerhalb des TGC, 2.) die Kontaktverhältnisse des TGC zu den umgebenden Metasedimentgesteinen und 3.) die Hochtemperaturscherzonen, die von einem Teilgebiet des TGC bekannt waren, zu untersuchen. Wir stellen hier die Ergebnisse der detaillierten Geländeuntersuchungen, von petrologischen Untersuchungen und von neuen geochronologischen Analysen vor. Basierend auf diesen Daten schlagen wir ein Modell vor, welches eine zweiphasige Entwicklung des TGC beinhaltet. Diese lässt sich zusammenfassen in: 1.) „Frühphase" (Maximalalter ca. 530 Ma) mit tektonomagmatischen Prozessen, die innerhalb der durch den TGC repräsentierten unteren Krustenbereiche des Bowers Terrane aktiv waren, und 2.) „Spätphase" (Maximalalter ca. 490 Ma), die der spät-Ross-orogenen Intrusion des TGC in die höherkrustalen metasedimentären Rahmengesteine des Bowers Terrane unter NE-SW gerichtetem horizontalem Hauptdruck sowie anschließender Abkühlung zugeordnet werden kann.

INTRODUCTION

Ultramafic to mafic complexes often mark sutures between collided continents or terranes. In northern Victoria Land (NVL) in Antarctica, the suture between the Wilson Terrane and the Bowers Terrane is marked by mafic to ultramafic intrusions, which bear valuable information on processes related to the magmatic evolution of island arc systems. These rocks are particularly wellsuited for evaluating the structural and geological evolution at the active continental margin of Palaeo-Victoria Land during the Cambrian (Rocchi et al. 1999, Capponi et al. 2003, Estrada & Jordan 2003, Rocchi et al. 2003, Tiepolo & Tribuzio 2008, Tribuzio et al. 2008).

There is currently a great interest in determining the origin of subduction-related mafic-ultramafic intrusive complexes. Unfortunately, these intrusions are rare and commonly volumetrically subordinate. It was suggested that they founder within the mantle because of their high density (for details see Behn & Kelemen 2006). Such intrusions are highly relevant to models for crustal development, because they potentially link upper mantle and lower crustal processes (Annen et al. 2006). Accordingly, understanding the emplacement and differentiation mechanisms of deep-seated magmatic bodies is crucial to understanding crustal growth mechanisms (DeBari 1994). Mafic and ultramafic intrusive rocks exposed along orogenic belts may thus be important sources of information on hidden crustal processes that occurred during subduction. Such rocks locally preserve relict mineral phases or complex zoning which is the record of variations in magma composition. Petrological results, when coupled with detailed geochronological data, can provide the timing of the different magmatic events and important constraints for the evolution of an orogen.

One of such suite of ultramafic-mafic, magmatic-arc related intrusives is the "Tiger Gabbro Complex" (TGC) at the southeastern termination and southwestern border of the Bowers Terrane in NVL (Ganovex Team 1987). The rocks of the TGC

[1] Bundesanstalt für Geowissenschaften und Rohstoffe (BGR), Stilleweg 2, D-30655 Hannover, Germany, <henjes-kunst@bgr.de>
[2] Institut für Mineralogie, Leibniz Universität Hannover, Callinstr. 3, D-30167 Hannover, Germany.
[3] Discipline of Earth Sciences, School of Environmental and Life Sciences, Science Building – SB110, The University of Newcastle, University Drive, Callaghan, NSW 2308, Australia.
[4] Geological Survey of New South Wales, 516 High Street, Maitland NSW 2320, Australia

Manuscript received 7 June 2014; accepted in revised form 21 October 2014.

are extraordinarily fresh and range from primitive olivine-pyroxene rich cumulates up to quartz-bearing diorites and anorthosites s.l.. In addition, in parts of the complex spectacular high-temperature shear zones are exposed. The present project was established to investigate the magmatic and structural evolution of the TGC by combining field work carried out during the GANOVEX X campaign in 2009/10 with geochronological and isotope geochemical analyses of samples taken during this expedition as well as from earlier GANOVEX campaigns. Our overarching aims for the project were: (i) to reconstruct the petrogenetic evolution of these cumulate rocks as a rare example of a deep-seated magmatic-arc related layered igneous complex, (ii) to investigate an affinity to either an oceanic or a continental magmatic-arc system and (iii) to provide insight into the final emplacement of the complex into its current structural position. The purpose of this paper, particularly, is to present field observations combined with first petrological and structural data as well as Ar-Ar age determinations. Results of ongoing isotope geochemical and geochronological studies and thermodynamic modeling will be published in later articles.

GEOLOGICAL BACKGROUND

The continental basement of NVL comprises three tectonic terranes (from SW to NE: the Wilson Terrane, the Bowers Terrane, and the Robertson Bay Terrane), which according to the model of KLEINSCHMIDT & TESSENSOHN (1987) were juxtaposed during the Cambro-Ordovician Ross Orogeny by accretionary processes above a westward dipping subduction zone (Fig. 1).

The Wilson Terrane represents the Palaeo-Pacific active continental margin of Gondwana. It mostly consists of low- to high-grade metasedimentary rocks (e.g., HENJES-KUNST & SCHÜSSLER 2003, HENJES-KUNST 2003) intruded by granitic to mafic plutons showing geochemical continental-arc affinity (Granite Harbour Intrusives; DI VINCENZO & ROCCHI 1999). The stratigraphically lower part of the Bowers Terrane is composed of intercalated low-grade metavolcanic and metasedimentary rocks that have traditionally been interpreted to represent a Middle to Late Cambrian intra-oceanic island arc (WEAVER et al. 1984). The metasedimentary rocks (Molar Formation) are turbiditic in nature and grade upwards into the shallow marine Mariner Formation. The upper part of the Bowers Terrane is built up by km-thick terrestrial deposits (Leap Year Group). The Robertson Bay Terrane is composed of turbiditic metasedimentary rocks of late Cambrian to Ordovician age (HENJES-KUNST & SCHÜSSLER 2003, HENJES-KUNST 2003). During the Ross Orogeny, accretion of the Bowers Terrane (together with the conjoined Robertson Bay Terrane to the east) to the eastern margin of the Wilson Terrane was accompanied by widespread folding and lower greenschist facies metamorphism. The suture zone between the Wilson and Bowers terranes, a key area for the construction of a geodynamic model for the Ross Orogeny in NVL (e.g., ROCCHI et al. 1999, ESTRADA & JORDAN 2003, ROCCHI et al. 2003, FEDERICO et al. 2006), is marked by the presence of mafic to ultramafic intrusions (Fig. 1). They have been interpreted to form the deeper crustal part of a juvenile magmatic-arc system of Cambrian age (TIEPOLO & TRIBUZIO 2008, TRIBUZIO et al. 2008).

One of these mafic bodies is the TGC, a layered intrusion located at the southeastern termination of the Bowers Terrane at the Ross Sea coast (Fig. 1). It crops out over an area of 35 km^2 at Dragontail Hills (southeastern Spatulate Ridge) and at Apostrophe Island (Fig. 2). Typical lithologies are pyroxenites, gabbros, gabbronorites, anorthosites s.l., and hornblende-plagioclase-rich pegmatoids (GANOVEX TEAM 1987, BRACCIALI et al. 2009). The complex exhibits well-exposed high-temperature shear zones. Geochronological data are scarce and generally not coherent. KREUZER et al. (1987) report a K-Ar age of 521 ±10 Ma on a hornblende from a pegmatoid. Subsequent Ar-Ar dating of this hornblende (RICCI & TESSENSOHN 2003) revealed two discrete plateau-like age intervals of 501 ±3 Ma, and 483 ±2 Ma, respectively. ROCCHI et al. (1999) and BRACCIALI et al. (2009) report a Sm-Nd isochron age of 535 ±21 Ma based on three whole-rock samples and an Ar-Ar step-heating age determination of a hornblende which again yields two discrete plateau-like age intervals of 510 ±10 Ma, and 499 ±6 Ma, respectively. Whole-rock trace-element geochemistry suggests a calc-alkaline character of the TGC (ROCCHI et al. 2003). More recent geochemical investigations and modeling (BRACCIALI et al. 2009) indicate a primitive low-K tholeiitic character and support the cumulate nature. Based on these data, BRACCIALI et al. (2009) interpret the TGC as a *"root of an island arc within the Palaeozoic margin of Gondwana"* and suggest a genetic link between the TGC and the metavolcanic rocks of the Cambrian Bowers Terrane.

From the study of the Bowers Terrane country rocks (Middle Cambrian Sledgers Group) to the north of the TGC, Engel (1987) reports a 4.5 km wide contact aureole with estimated temperatures of 800 °C at pressures of 0.2-0.4 GPa close to the contact. However, the contact between the TGC and metasedimentary and metavolcanic rocks of the Bowers Terrane remains a matter of discussion since it is only exposed in two steep cliffs at the northwestern and northeastern margins of the TGC (Fig. 2) which are not easily accessible. Based on helicopter-supported fieldwork, CAPPONI et al. (2003) and BRACCIALI et al. (2009) suggest that the contact between the TGC and the Bowers Terrane metasedimentary and metavolcanic rocks is of tectonic origin.

Geochemical and geochronological investigations also exist for two other mafic-ultramafic igneous complexes at the suture between the Wilson and Bowers terranes. The Niagara Icefall Intrusion (Fig. 1) is composed of pyroxenites, gabbronorites, ferrogabbronorites of cumulate origin with boninitic affinity (TRIBUZIO et al. 2008). From U-Pb zircon dating, a formation age of 514 ±2 Ma was concluded. According to TRIBUZIO et al. (2008), the Niagara Icefalls suite represents an igneous complex formed in an embryonic back-arc basin at the active continental margin of Gondwana in the Middle Cambrian. For the other mafic complex, the Husky Ridge Intrusion (Fig. 1), TIEPOLO & TRIBUZIO (2008) report the dominance of quartz diorites and amphibole-rich cumulates with sanukitic affinity (related to melts which originated by equiliration of subduction-derived sediment melts with a refractory mantle). From in-situ U-Pb geochronology on zircon grains, an age of 516 ±3 Ma was extracted, which is within its error limits identical to the age of the Niagara Icefall intrusion.

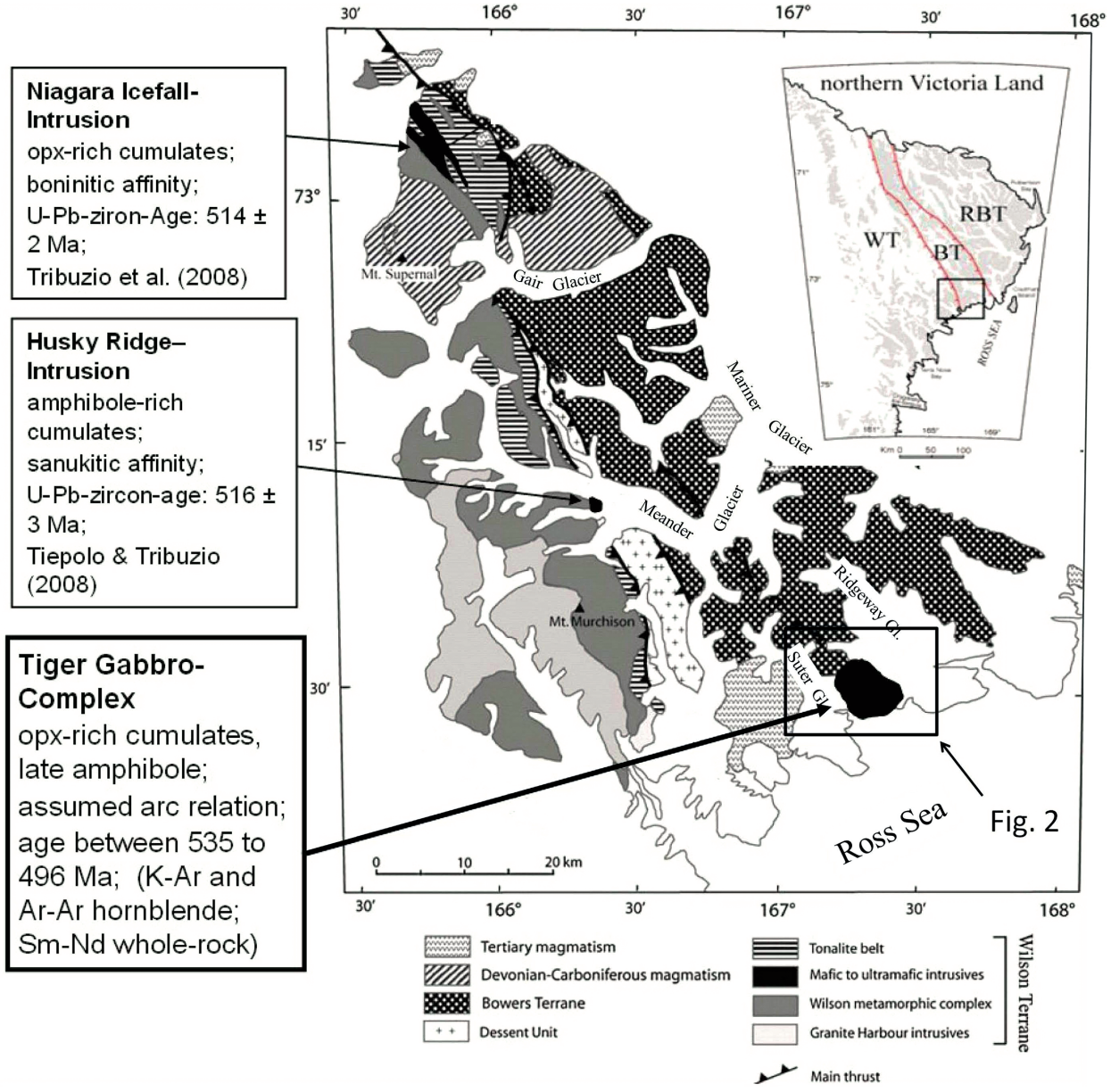

Fig. 1: Mafic to ultramafic igneous complexes with magmatic-arc relation at the suture between the Wilson and Bowers terranes. Map from TRIBUZIO et al. (2008). Inset northern Victoria Land: WT = Wilson Terrane; BT = Bowers Terrane; RBT = Robertson Bay Terrane. Tiger Gabbro Complex is located between the ice tongues of the Suter Glacier and the Ridgeway Glacier at the southeastern end of the Bowers Terrane.

Abb. 1: Mafische bis ultramafische Komplexe mit Inselbogenaffinität entlang der Sutur zwischen dem Wilson und Bowers Terrane. Karte von TRIBUZIO et al. (2008). Inset-Karte northern Victoria Land: WT = Wilson Terrane, BT = Bowers Terrane, RBT = Robertson Bay Terrane. Lage des Tiger Gabbro Complex zwischen den Eiszungen von Suter Glacier und Ridgeway Glacier am Südostende des Bowers Terrane.

OBJECTIVES OF A DETAILED INVESTIGATION OF THE TIGER GABBRO COMPLEX (TGC)

The TGC has the potential (i) to provide key information on hidden crustal processes that occurred during subduction along the eastern margin of Gondwana in the early Palaeozoic, and (ii) to provide general knowledge on details of the magmatic evolution and petrogenesis of island arcs. As mentioned above, published scientific results are rare, highly incomplete and leave open many questions, such as:

(i) What characterizes the lithological and geochemical diversity of the TGC? So far, only geochemical data for 10 whole-rock samples and trace-element data for 5 samples are published.

(ii) What characterizes the mineralogical diversity of the TGC? Earlier studies do not present a systematic description on the mineralogy of the compositional layering.

(iii) What is the formation age of the complex? The available geochronological data do not yield consistent age constraints because of methodical shortcomings. With respect to the Sm-Nd whole-rock age, there is no proof of initial Nd isotope equilibration in the complex based on the analysis of three samples only. Furthermore, the published Ar-Ar age determinations on hornblende yielded age spectra, which do not allow for a straightforward geological interpretation.

(iv) What is the composition of the parent melt(s)? The interpretation of BRACCIALI et al. (2009) is based on the modeling results performed on three samples only.

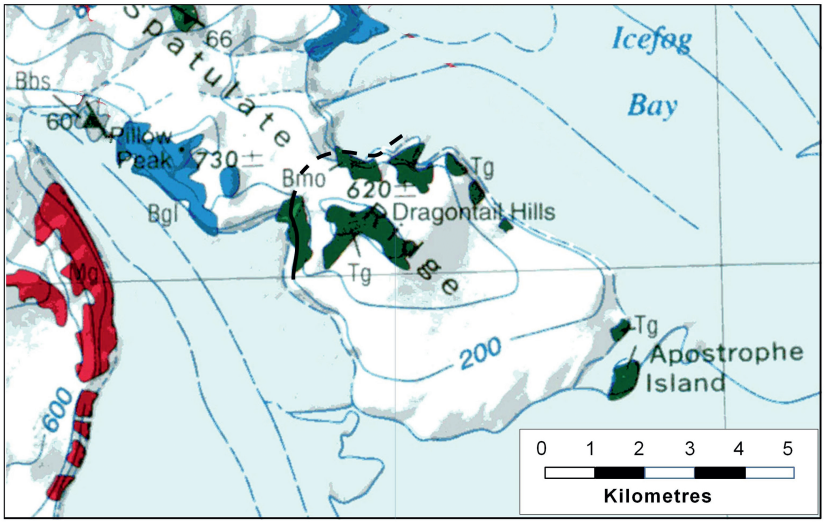

Fig. 2: Geological map of the area under investigation showing the outcrops of the Tiger Gabbro Complex ("Tg") in dark green (modified after CAPPONI et al. 1997). Outcrops of the TGC are known from the area of Dragontail Hills, southeastern end of Spatulate Ridge, and from Apostrophe Island to the southeast. The contact to metasedimentary rocks of the Bowers Terrane ("Bmo" in green) forming the country rocks to the NW is indicated by a black solid line. The contact to the north (dashed black line) is extrapolated from helicopter-based survey. Metavolcanic rocks of the Bowers Terrane ("Bgl") in blue; Cenozoic igneous rocks ("Mg") in red.

Abb. 2: Geologische Karte mit den Aufschlüssen des Tiger Gabbro Complex („Tg") in dunkelgrün (modifiziert nach CAPPONI et al. 1997). Aufschlüsse im TGC sind bekannt aus der Gegend Dragontail Hills, Südosten von Spatulate Ridge und von Apostrophe Island im Südosten des Gebietes. Der direkte Kontakt zu den metasedimentären Nebengesteinen des Bowers Terrane („Bmo" in hellgrün) im nördlichen Teil des TGC ist schwarz eingezeichnet (durchgezogene Linie = besucht; gestrichelt = extrapoliert nach Beobachtungen aus dem Hubschrauber). Metavulkanite des Bowers Terrane („Bgl") in blau; känozoische Magmatite („Mg") in rot.

Therefore, it is our attempt to establish a detailed petrogenesis of the TGC including its magmatic evolution, subsolidus cooling path, and high-temperature shearing history, with the aim to evaluate the geological evolution of deep crustal sequences supposed to have formed the root of an island-arc system. Here, we present the first results of petrographic investigations performed on samples collected during earlier GANOVEX campaigns, the results of the field work in the TGC in the frame of the GANOVEX X campaign and the results of preliminary geochronological investigations (Ar-Ar dating on amphibole). Building on the results of these first steps, we aim to conduct further investigations, which will include detailed (isotope) geochemical and geochronological studies and experimental modeling of the TGC.

RESULTS OF PRELIMINARY PETROGRAPHICAL INVESTIGATIONS

The work on the project was started in late 2009. From the rock repository of the Federal Institute for Geosciences and Natural Resources (BGR), a collection of about 20 samples of the Tiger Gabbro Complex (collected during GANOVEX III in 1982/83) was found suitable for petrographical, geochemical and in part microanalytical investigations.

Typical rocks of the TGC are gabbronorites, gabbros, anorthosites, pyroxenites, hornblende diorites, and hornblendites in order of decreasing abundance. They are characterized petrographically in the following.

• Gabbronorites to gabbros form by far the largest group among the plutonic rocks from the TGC (see below). They are mostly medium grained, granular rocks with subhedral crystal shapes (Figs. 3a, b). Those rocks sampled in the layered series of Dragontail Hills show a strong magmatic foliation, other rocks are isotropic. Beside plagioclase, clino- and orthopyroxene forming the principal phases, olivine, pargasite, and Fe-Ti oxides are present in minor amounts. Some rocks bear relatively high amounts of Fe-Ti oxides (max 5 vol.%) leading to the evolution of ferrogabbronorites. Pargasite always crystallized late, forming interstitial assemblages, often associated with Fe-Ti oxides. In one sample, small seams of orthopyroxene are visible surrounding olivine. Most rocks show signs of deformation, as cataclastic zones cutting the rocks, bands of fluid inclusions in the principal minerals, undulose extinction, and plastic deformation mostly recorded in bent plagioclases.

• Anorthosites are medium grained, isotropic rocks with granular texture and anhedral mineral shapes, bearing more than 95 vol.% plagioclase (Figs. 3c, d); the rest is composed of pargasite, oxide, and clinopyroxene. A record of deformation both in plastic and brittle regimes is present (bent plagioclase lamellae, cataclastic zones, undulose extinction).

• Pyroxenites are medium to coarse grained rocks consisting mainly of clinopyroxene and orthopyroxene (>90 vol.%) with additional pargasite, oxide, plagioclase in amounts <5 vol.% for each phase (Figs. 3e, f). The textures are granular, equigranular to seriate, mostly with subhedral mineral shapes. These rocks show in part a tectonic overprint both in the plastic and brittle regimes leading to mylonitic and cataclastic domains, respectively. Exsolution lamellae of orthopyroxene in clinopyroxene and vice versa are common. Some pyroxenes show shear-related bands of fluid inclusions implying that the shear process was associated with a fluid phase.

• Hornblende diorites are evolved rocks composed mainly of plagioclase and amphibole, associated with additional phases in minor amounts like clino- and orthopyroxene, oxide and quartz (Figs. 3g, h). Their textures are medium grained, granular, isotropic with subhedral crystal shapes. Signs of deformation both in the plastic and in the brittle regime are always visible (bent plagioclase lamellae, cataclastic bands, undulose extinction). While most gabbroic rocks of the TGC are very fresh, the hornblende diorites show a strong alteration (high amounts of chlorite, secondary albite).

• Gabbros s.l. sampled close to the high-temperature shear zones at Apostrophe Island typically show a porphyroclastic texture, expressed by mm- to cm-sized pyroxene and olivine porphyroclasts swimming in fine grained to cryptocrystalline mylonitic or cataclastic matrix (Figs. 3i, j). Neoblasts of the matrix and of domains surrounding the porphyroclasts show a granoblastic network, which includes also pargasite and Fe-Ti oxides (Fig. 3k). The porphyroclasts may bear bands of fluid

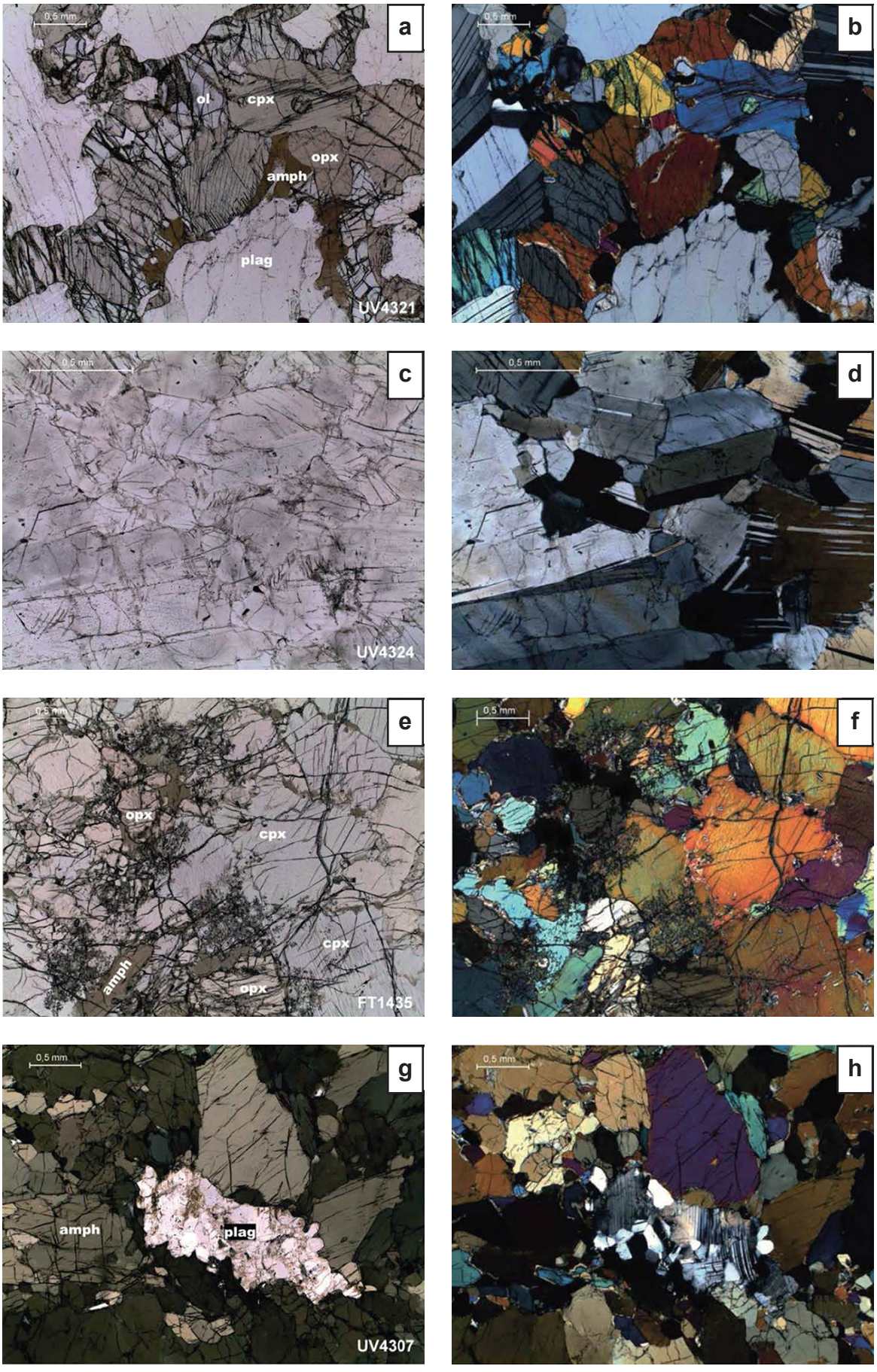

Fig. 3 / Abb. 3 continued ▶

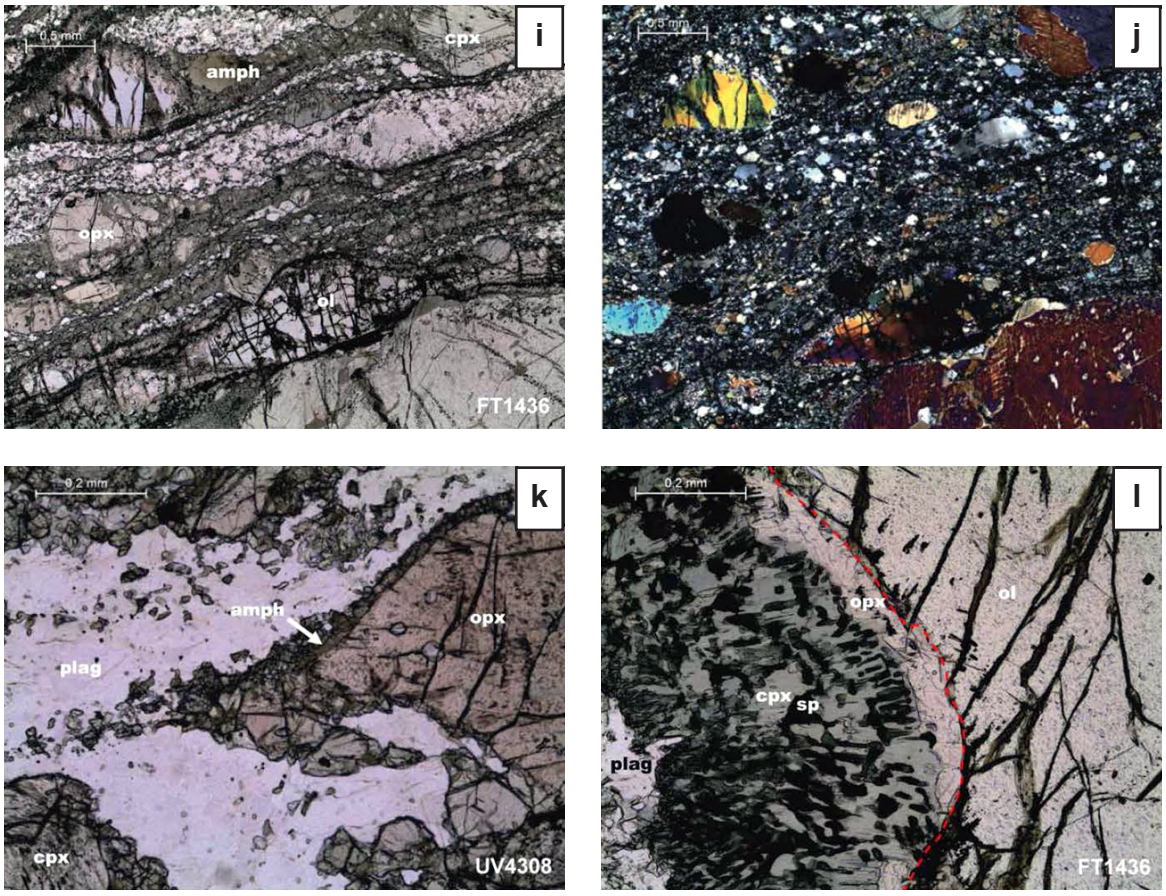

Fig. 3 a-l: Microphotographs of thin sections of samples of the Tiger Gabbro Complex from the BGR sample repository collected by F. Tessensohn and U. Vetter during GANOVEX III in 1982/83. Abbreviations: cpx = clinopyroxene, opx = orthopyroxene, ol = olivine, amph = amphibole, sp = spinel. (a, b) = sample UV4321 (Dragontail Hills): olivine-bearing primitive gabbronorite. Olivine, orthopyroxene, and clinopyroxene form mafic clusters; the textural relations imply the crystallization order ol > plag > opx = cpx > amph. a = plane-polarized light; b = cross-polarized light. (c, d) = sample UV4324 (Dragontail Hills): anorthositic gabbro. Plagioclase shows a pronounced foliation probably due to magmatic "sedimentation" or flow processes in the magma chamber and plastic deformation indicating high-temperature shearing under sub-solidus conditions; c = plane-polarized light; d = cross-polarized light. (e, f) = sample FT1435 (Apostrophe Island): pyroxenite showing characteristic cumulate structure of the more primitive rocks, suggesting co-crystallization of opx and cpx, and late crystallization of amph in the interstices; e = plane-polarized light; f = cross-polarized light. (g, h) = sample UV4307 (Apostrophe Island): the presence of nearly monomineralic hornblendite (>95 % amph) documents accumulation processes of hornblende in a hydrous magma chamber, implying that under certain circumstances (pressure, water activity, bulk composition) amph was on the liquidus; g = plane-polarized light; h = cross-polarized light. (i, j) = sample FT1436 (Apostrophe Island): gabbronorite from a mylonitic to ultramylonitic high-temperature shearzone. The rock shows marked porphyroclastic textures with porphyroclasts of ol, opx, cpx, and amph and a mylonitic to neoblastic matrix; i = plane-polarized light; j = cross-polarized light. (k) = Sample UV4308 (Apostrophe Island): detail of a mylonitic to ultramylonitic gabbronorite. The fine-grained, recrystallized granulitic matrix is composed of opx, cpx, plag, and amph. Amph forms fine granoblastic networks enclosing tiniest opx and cpx, indicating hydrous conditions during the high-T-shearing process; plane-polarized light. (l) = sample FT1436 (Apostrophe Island): symplectitic intergrowths of sp and cpx boarded by a thin seam of opx (boundary towards ol is marked by a dashed line in red) as reaction products between primary magmatic ol and plag, interpreted as the record of sub-solidus processes during cooling; plane-polarized light.

Abb. 3 a-l: Dünnschliff-Fotografien von Proben des Tiger Gabbro Complex aus dem BGR Probenarchiv. Die Probennahme erfolgte durch F. Tessensohn und U. Vetter während GANOVEX III (1982/83). Abkürzungen: cpx = Klinopyroxen, opx = Orthopyroxen, ol = Olivin, amph = Amphibol, sp = Spinell. (a, b) = Probe UV4321 (Dragontail Hills): Olivin-haltiger primitiver Gabbronorit. Olivin, Orthopyroxen und Klinopyroxen bilden mafische Anhäufungen, die von relativ spät auskristallisiertem, oft in Zwischenräumen vorliegendem Amphibol umgeben sind. Die Gefügebeziehungen implizieren eine Kristallisationsabfolge ol > plag > opx = cpx > amph; a = linear-polarisiertes Licht; b = gekreuzt-polarisiertes Licht. (c, d) = Probe UV4324 (Dragontail Hills): Anorthositischer Gabbro. Plagioklas mit deutlicher Foliation vermutlich aufgrund magmatischer "Sedimentation" oder Fließprozessen in der Magmenkammer und plastische, subsolidus Verformung infolge hochtemperierter Scherprozesse; c = linear-polarisiertes Licht; d = gekreuzt-polarisiertes Licht. (e, f) = Probe FT1435 (Apostrophe Island): Pyroxenit mit charakteristischen Kumulatstrukturen der primitiveren Gesteine, welcher gleichzeitige Kristallisation von Ortho- und Klinopyroxen und späte Kristallisation von Amphibol in den Zwischenräumen vermuten lässt; e = linear-polarisiertes Licht; f = gekreuzt-polarisiertes Licht. (g, h) = Probe UV4307 (Apostrophe Island): Das Auftreten von fast monomineralischen Hornblenditen (>95 % Amphibol) dokumentiert Akkumulationsprozesse von Hornblende in einer wasserreichen Magmenkammer und belegt, dass unter besonderen Umständen (Druck, Fluidaktivität, Gesamtzusammensetzung) Amphibol auf dem Liquidus liegt; g = linear-polarisiertes Licht; h = gekreuzt-polarisiertes Licht. (i, j) = Probe FT1436 (Apostrophe Island): Mylonitische bis ultramylonitische Hochtemperatur-Scherzone in einem Gabbronorit. Die Gesteine zeigen oft auffällige porphyroklastische Texturen mit Porphyroklasten aus Olivin, Orthopyroxen, Klinopyroxen und Amphibol und eine mylonitisch bis neoblastische Matrix; i = linear-polarisiertes Licht; j = gekreuzt-polarisiertes Licht. (k) = Probe UV4308 (Apostrophe Island): Detail eines mylonitisch bis ultramylonitischen Gabbronorits. Die feinkörnig rekristallisierte granulitische Matrix besteht aus Orthopyroxen, Klinopyroxen, Plagioklas und Amphibol. Der Amphibol bildet ein feinkörnig-granoblastisches Netzwerk, das sehr feinkörnige Pyroxene einschließt, und damit auf erhöhte Fluidaktivität während des hochtemperierten Scherprozesses hindeutet; linear-polarisiertes Licht. (l) = Probe FT1436 (Apostrophe Island): Symplektitische Verwachsungen von Spinell und Klinopyroxen mit dünnem Saum aus Orthopyroxen zu Olivin (die Grenze zum Olivin ist durch eine rot-gestrichelte Linie gekennzeichnet) als Reaktionsprodukte zwischen primärmagmatischem Olivin und Plagioklas, was als Hinweis auf Subsolidusprozesse während der Abkühlung gedeutet wird; linear-polarisiertes Licht.

inclusions, implying, together with the presence of amphibole in the neoblastic domains, that during the recrystallization processes under deformative conditions, a fluid-rich phase was present. Some porphyroclastic to mylonitic gabbros show characteristic reaction products between primary magmatic olivine and plagioclase consisting of thin orthopyroxene seams next to olivine and symplectitic intergrowths of spinel and clinopyroxene next to plagioclase, interpreted as the record of sub-solidus processes during cooling (Fig. 3l). Identical features were observed in gabbros from the Chilas Complex (Kohistan, NW Pakistan), which is regarded as world site for island-arc gabbros in the deep crust of a juvenile island arc (JAGOUTZ et al. 2007).

Microprobe analyses were performed on the rock-forming silicate minerals and in part oxide phases of selected samples using the Cameca SX 100 electron microprobe at the Institute for Mineralogy, Leibniz University Hannover. Details on the conditions of measurements can be found in Koepke et al. (2011). Data are archived in the database "PANGAEA" (http://doi.pangaea.de/10.1594/PANGAEA.810354) and presented in Table 1. The mineral analyses are presented complementary to the petrographical description of the major rock types but will not discussed in detail here.

Our petrographic characterization indicates that the TGC provides an ideal suite of rocks to achieve the goals of the project. First-order observations on different aspects of the petrogenesis of the TGC are:
(i) The presence of a whole suite of crystallization products from early cumulates (olivine-bearing pyroxenites) to chemically highly evolved rocks (anorthosites s.l.), enabling the possibility to establish the magmatic evolution.
(ii) The crystallization order: in pyroxenitic cumulates plagioclase crystallizes after pyroxene, while in gabbronorites plagioclase crystallizes before.
(iii) The dominance of gabbronoritic lithologies.
(iv) The role of amphibole which may form true cumulate rocks (hornblendites), poikilitic clusters, or interstitial crystals. Some amphiboles are definitely of magmatic origin, others can be interpreted as formed at subsolidus conditions.
(v) The record of significant high-temperature shear processes expressed by spectacular porphyroclastic to mylonitic textures in samples from Apostrophe Island. Samples with porphyroclastic to mylonitic textures are observed in different lithologies of the TGC at Apostrophe Island spatially not related to each other and thus indicate that the high-temperature shear processes are likely not related to a pervasive post-magmatic deformation event.
(vi) A well-developed cooling history. Some gabbros show characteristic symplectitic intergrowths, interpreted as the record of sub-solidus processes during cooling. Exsolution lamellas of orthopyroxene in clinopyroxene and vice versa are also common.

RESULTS OF FIELD WORK DURING GANOVEX X

Fieldwork conducted during GANOVEX X (2009/10) shows that gabbronorites s.l. and leucocratic plagioclase-rich cumulate rocks comprise the majority of the Dragontail Hills (southeastern Spatulate Ridge) whereas ultramafic cumulate rocks with very low plagioclase content are dominant at Apostrophe Island. At both localities, chemically evolved alkali feldspar-bearing igneous rocks, which are known as late differentiates from other well-studied layered intrusions like the Bushveld and Stillwater complexes, are absent. The gabbronorites s.l. at Dragontail Hills show well exposed rhythmic or intermittent layering that dips between 45° and 65° toward the southwest (Fig. 4a). Cross-bedding relationships were found (Fig. 4b). Thickness of the individual layers ranges from centimeter to meter. Compositionally, the layers vary between melanocratic gabbronoritic rocks that are low in plagioclase content and very leucocratic rocks composed almost exclusively of plagioclase (anorthosites s.l., Fig. 4c). Layers may either show graded variations in modal composition or uniform compositions. In addition, there are lenses of ultramafic rocks up to several hundred meters long orientated roughly parallel to the magmatic layering. Their thickness is generally less than hundred meters. Due to stronger weathering of the ultramafic rocks, no in-situ contact to the layered gabbronorites could be identified. However, based on the overall layered character of the whole sequence and the absence of intrusive relationships between the ultramafic rocks and the gabbronorites s.l. at Dragontail Hills, it is assumed that both form part of one major layered igneous sequence ("layered unit") which bears many similarities to banded series of large layered intrusions like the Bushveld, Stillwater or Skaergaard complexes. Especially the rhythmic and/or intermittent layering can only be explained by processes of crystallization, differentiation and layering typical for magma chambers of layered mafic intrusions (e.g. WINTER 2001).

The ultramafic rocks at Apostrophe Island do not show obvious layering. There is, however, clear evidence of interaction between these rocks and gabbronoritic rocks similar to those exposed at Dragontail Hills – but here without the characteristic igneous layering – from magma mixing/mingling relations between the two (Figs. 4d-f). The gabbronoritic rocks show intrusive contacts towards the ultramafic rocks and contain blocky to rounded enclaves and schlieren of ultramafic rocks. The enclaves either have sharp contacts or their margins are partially disintegrated and mixed up with gabbroic material (Fig. 4e). Very similar magma mixing/mingling relations between ultramafic cumulates and gabbroic to more evolved igneous rocks were described from other intrusive complexes in northern Victoria Land (e.g., at Teall Nunatak, southern Wilson Terrane; GIACOMINI et al. 2007). These structures indicate that emplacement of both rock types occurred nearly contemporaneously while they were still in a (partially) molten state. With respect to the dominance of ultramafic lithologies, the TGC at Apostrophe Island corresponds to the basal series of well characterized layered intrusions like the Bushveld or Stillwater complexes.

Localized high-temperature and high-strain shear zones were identified along the northern margin of Apostrophe Island at 73°31'05" S, 167°26'05" E. These shear zones range from narrow (<10 cm) planar low-angle mylonitic to wide (2-4 m) cataclastic shear zones. They are associated with synkinematic injections of plagioclase and phenocrystic hornblende-rich melts (Figs. 5a, b). Larger shear zones have formed by duplexing, with these melts injected along the dominant main deformation zones and from there into associated joint systems within the rock (Fig. 5b). Geometrically, the shear zones strike southeast–northwest (135-150°) and dip shallowly (25-40°)

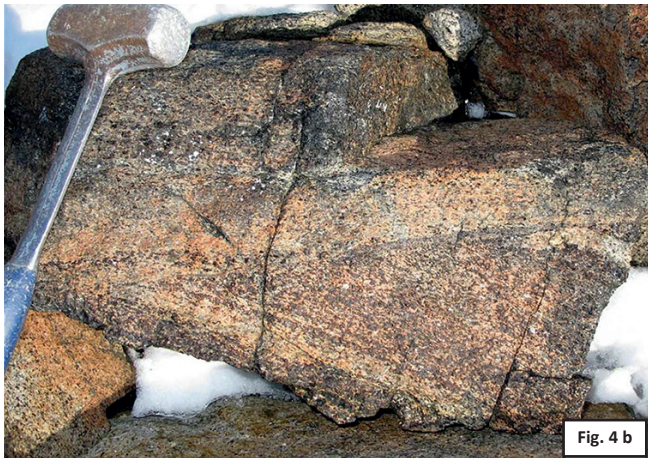

Fig. 4 a-c: Field photographs of the Tiger Gabbro Complex (TGC). (a) = Tiger Gabbro from Dragontail Hills showing typical rhythmic to intermittent and in part graded layering on a cm scale; see hammer for scale. (b) = Magmatic crossbedding in TGC at Dragontail Hills; hammer for scale. (c) = Layering of very leucocratic rocks at Dragontail Hills. Modal composition varies between plagioclase-rich layers low in contents of mafic minerals (anorthositic gabbro) to nearly monomineralic anorthosite s.l.; hammer for scale. (d) = Ultramafic rocks (pale green) at Apostrophe Island intruded by and reacting with hornblende-plagioclase-rich melts (dark coloured) originating from the high-strain shear zone in the lower left of the photograph; see ice axe for scale. (e) = Relationships between dark coloured ultramafic rocks and lighter coloured gabbronoritic rocks resulting from magma mingling and mixing, see Figure 4 f for details; ice axe for scale. (f) = Schlieren of dark coloured ultramafic material in a lighter coloured gabbronoritic matrix bearing clear evidence of interaction of two magmas with different chemical and physical properties; ice axe for scale.

Abb. 4 a-c: Geländefotografien des Tiger Gabbro Complex (TGC). (a) = Tiger Gabbro von Dragontail Hills mit typischem rhythmischem bis wechsellagerndem und teilweise gradiertem Lagenbau im cm-Bereich; Hammerstiel als Maßstab. (b) = Magmatische Schrägschichtung im TGC bei Dragontail Hills; Hammer als Maßstab. (c) = Lagenbau in sehr leukokraten Gesteinen bei Dragontail Hills. Die modale Zusammensetzung variiert von Plagioklas reichen Lagen mit niedrigem Anteil an mafischen Mineralen (anorthositischer Gabbro) zu fast monomineralischen Anorthositen s.l.; (Hammer als Maßstab). (d) = Ultramafite (blass grün) auf Apostrophe Island, welche von Hornblende-Plagioklas reichen Schmelzen intrudiert und assimiliert werden. Die Hornblende-Plagioklas reichen Schmelzen entstammen der Hochtemperaturscherzone links unten im Bild; (Eispickel als Maßstab). (e) = Beziehungen zwischen dunklen ultramafischen Gesteinen und helleren gabbronoritischen Gesteinen, die aus Vermischungsprozessen des Magmas resultieren, weitere Details siehe Abbildung 4 f; Eispickel als Maßstab. (f) Schlieren aus dunklem ultramafischem Material in einer helleren gabbronoritischen Matrix geben Hinweis auf Interaktionen zweier Magmen mit unterschiedlichen chemischen und physikalischen Eigenschaften; Eispickel als Maßstab.

toward the northeast (Fig. 5c). A consistent lineation defined by elongate hornblende, epidote and chlorite crystals that shallowly plunge (20-40°) to the northeast (50-65°) indicates the direction of transport along the shear planes. Kinematic indicators include crystal-plastic structures with S-C relationships in the high-strain internal parts of the shear zones, dilational 'lock-up' structures and late-stage brittle structures such as Riedel shears. Crystal-plastic deformation of plagioclase and hornblende suggests minimum temperatures of 650-700 °C (e.g., PASSCHIER & TROUW 2005 and references therein). All these fabrics consistently indicate a reverse, top-to-SW directed sense of transport on the shear zones. Localized folding was also identified. Folds are open to closed and asymmetrically verge to the south. Fold hinges shallowly plunge to the northeast (~35° to 75°), with axial surfaces dipping moderately (~50°) to the southeast (~115°). Perpendicular to the shear zones are high-angle semi-brittle tension gashes, which are also filled by the plagioclase-hornblende-rich melts (Fig. 5a). The tension gashes strike southeast–northwest (~150°) and dip steeply (75°) to the southwest. As a result, it can be assumed that the high-temperature shear zones and the tension gashes formed nearly synchronously under localized very high strain. Equilibrium temperatures were calculated for the granulite-facies mylonitic matrix (Figs. 3i, j) of a porphyroclastic gabbro (FT1436) from a high-strain shear zone at Apostrophe Island to c. 800 °C based on the Ti-in-amphibole thermometer (ERNST & LIU 1998) and to c. 855 °C based on the hornblende-plagioclase thermometer (HOLLAND & BLUNDY 1994). A prerequisite for applying the Ti-in-amphibole thermometer is that the amphibole must coexist with a titanian phase. This is given in sample FT1436 where pargasite in the neoblastic matrix forms an equilibrium assemblage together with ilmenite. This geothermometer is regarded as semi-quantitative, but the application to gabbroic rocks was confirmed experimentally by KOEPKE et al. (2003).

Large elongated hornblende crystals within the shear zone shown in Figure 5b were dated by the Ar-Ar method (sample TG 101, Fig. 6). The sample yielded an age spectrum with a well defined high temperature four steps plateau characterized by 96.3 % of the released ^{39}Ar and an age value of 518.6 ±4.6 Ma. The geological significance of this Ar-Ar age is, however, unclear. It is well known that minerals formed in shear zones may contain radiogenic Ar not related to in-situ decay of K ("excess Ar", MCDOUGALL & HARRISON 2000). The excess Ar is related to radiogenic Ar released from sheared country rocks. Since the amount of likely excess Ar in a mineral with plateau-like age spectrum cannot be quantified, the c. 519 Ma age for amphibole TG 101 can only be regarded as a maximum formation age. Two further Ar-Ar analyses were

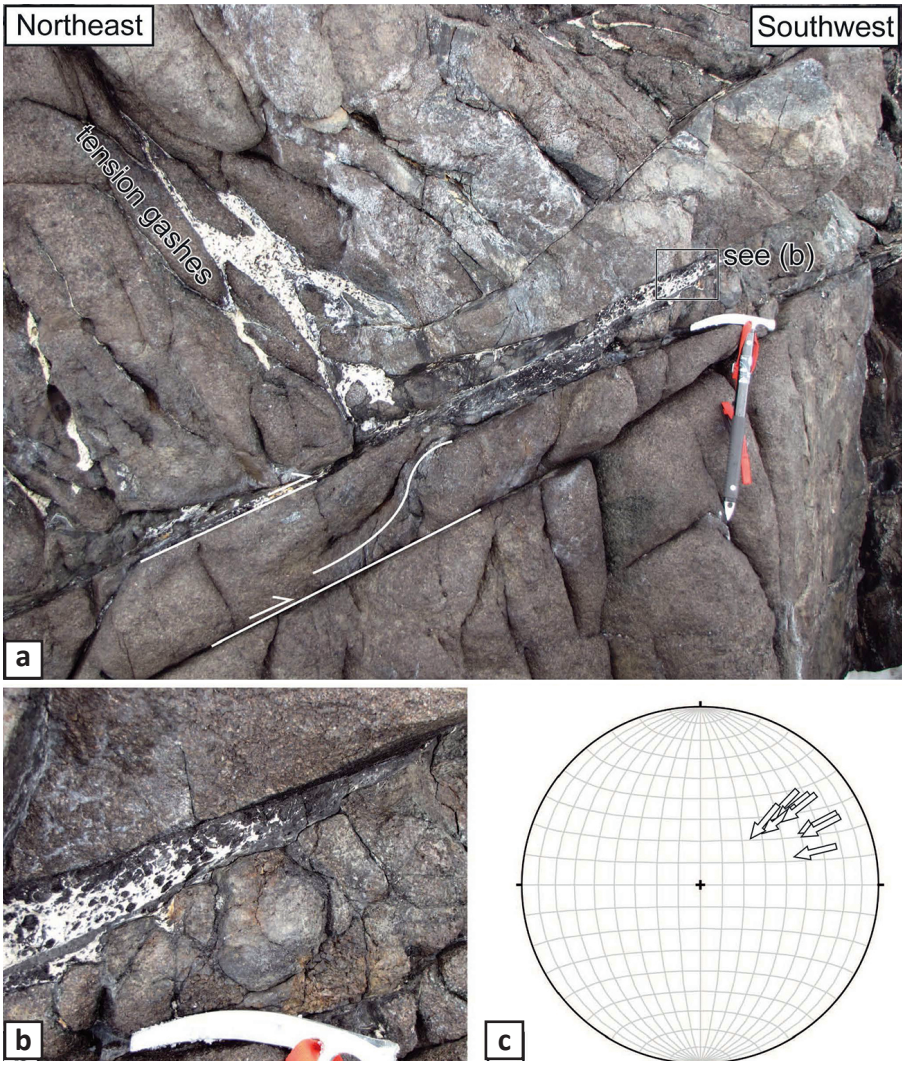

Figs. 5 a-c: Field photographs and structural data of a shear zone in the Tiger Gabbro Complex at Apostrophe Island. (a) = Low-angle reverse high-strain shear zone located at Apostrophe Island. S-C relations (with large hornblende crystals in S-position) confirm a reverse sense of transport. Tension gashes formed at high angles to the main shear zone are filled with plagioclase-hornblende melt injections. (b) = Close up of plagioclase-hornblende melt injected along the main shear plane. (c) = Equal area stereographic projection of hanging-wall transport vectors for high-strain zones identified at Apostrophe Island.

Abb. 5 a-c: Geländefotografien und Strukturdaten einer hochtemperierten Scherzone im Tiger Gabbro Complex bei Apostrophe Island. (a) = Flach einfallende, aufschiebende hochtemperierte Scherzone bei Apostrophe Island. S-C Gefüge (große Hornblende-Kristalle in S-Position) belegen den aufschiebenden Bewegungssinn. Dehnungsklüfte stehen in großem Winkel zur Hauptscherzone und sind gefüllt mit Plagioklas-Hornblende reichen Schmelzinjektionen. (b) = Nahaufnahme einer Plagioklas-Hornblende-reichen Schmelze, welche entlang der Scherzone injiziert ist. (c) = Stereographische Projektionen (untere Halbkugel) der Bewegungsvektoren des hangenden Blocks in den hochtemperierten Scherzonen von Apostrophe Island.

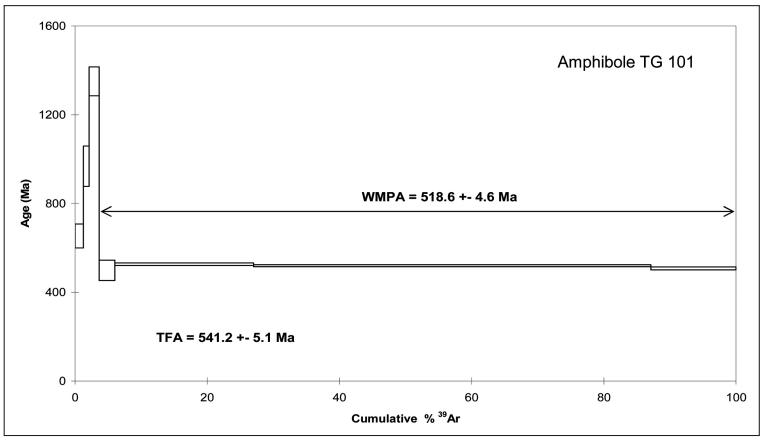

Fig. 6: Ar-Ar age spectrum of large hornblende crystals from the high-temperature shear zone at Apostrophe Island (see Fig. 5b); analyses performed by Actlabs (Canada).

Abb. 6: Ar-Ar Altersspektrum von großen Hornblenden aus der Hochtemperatur-Scherzone von Apostrophe Island (siehe Abb. 5b); Analysen durch Actlabs (Kanada).

performed on amphiboles separated from the TGC (Fig. 7). Sample UV4307 is a plagioclase hornblendite from Apostrophe Island. Hornblende crystals separated from this sample gave an age of 529.7 ±4.3 Ma. However, since the data points defining this age yield no isochron in the inverse isochron plot, this datum should also be interpreted with caution and can give only a rough age trend for the TGC. The second sample UV4335 represents a hornblende diorite from Dragontail Hills. Its amphibole yielded a spectrum with an age of 504.7 ±3.7 Ma.

The contact of the TGC to the country rocks of the Bowers Terrane was examined at a cliff on the northwestern side of Dragontail Hills. Here, gabbronoritic rocks of the layered unit of the TGC were found in contact to strongly contact-metamorphosed metasedimentary rocks of the Bowers Terrane approximately 75 m (GPS values) below the upper edge of the cliff (Fig. 8a). Close to the contact, the gabbronoritic rocks include small lenses of the metasedimentary country rock (Fig. 8b). There is no evidence for deformation neither in the gabbronorite nor in the country rock as would be expected for a tectonic emplacement of the TGC according to Capponi et al. (2003) and Bracciali et al. (2009). The metasedimentary rock exhibits abundant discontinuous and strongly welded quartz mobilisates in a zone, which extends several 10 metres away from the contact. Welding is highly chaotic (Fig. 8c) probably

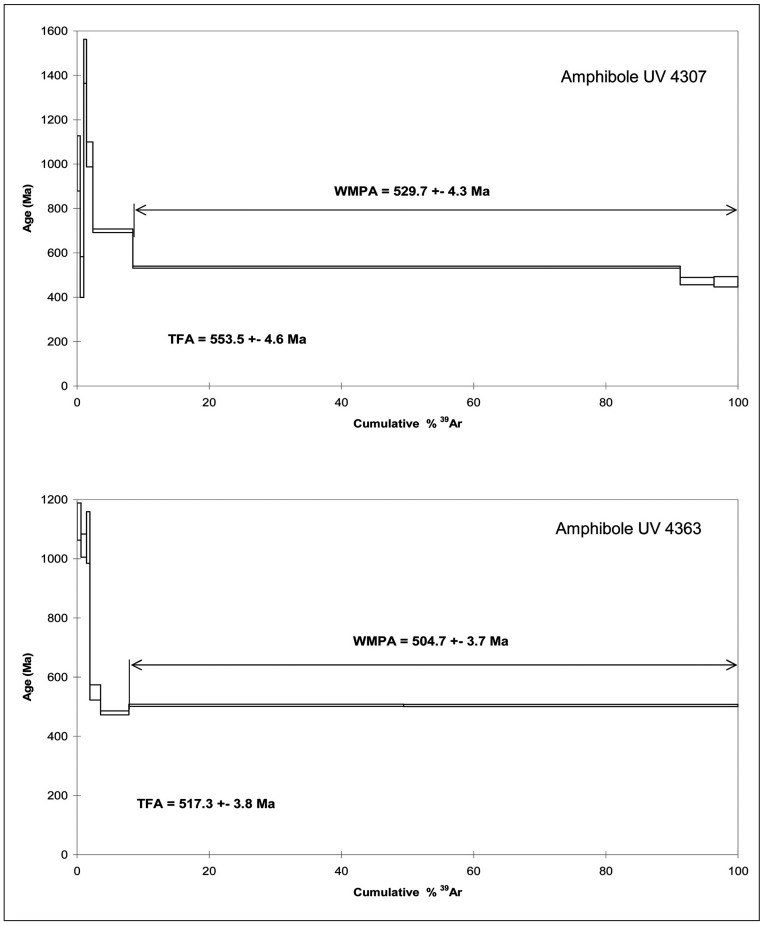

Fig. 7: Ar-Ar age spectra of amphiboles separated from a plagioclase hornblendite (UV 4307, top) from Apostrophe Island and from a hornblende diorite from Dragontail Hills (UV 4363, bottom); analyses by Actlabs (Canada).

Abb. 7: Ar-Ar Altersspektren von Amphibolen aus einem Plagioklas-Hornblendit (UV 4307, oben) von Apostrophe Island und einem Hornblende-Diorit von Dragontail Hills (UV 4363, unten); Analysen durch Actlabs (Kanada).

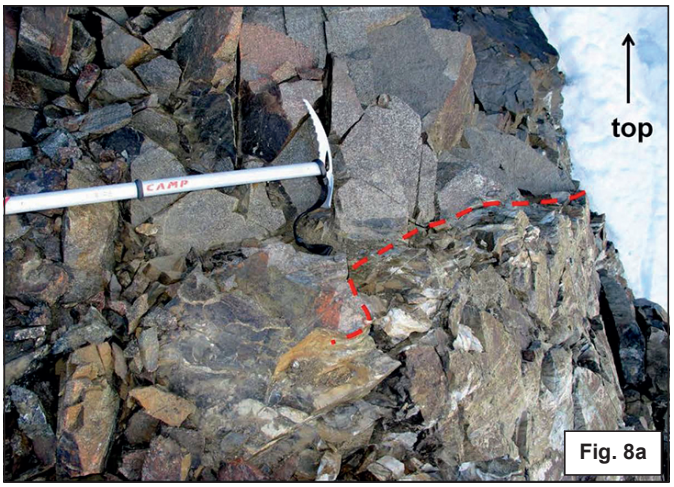

Figs. 8 a-c: Contact relationship between the Tiger Gabbro complex and metasedimentary rocks in a cliff at the northwest side of Dragontail Hills. (a) = Photograph of the contact (top: gabbroic rocks of the Tiger Gabbro Complex; bottom: metasedimentary rocks of the Bowers Terrane; ice axe for scale). The contact is marked by a red dashed line. At the left end of the dashed line, the contact is characterized by a mélange made up to about 90 % by lenses of metasedimentary rocks veined by gabbroic material (about 10 %). (b) = Lenses and schlieren of country rock in an undeformed gabbronorite from the contact of the TGC to metasediments of the Bowers Terrane (hammer for scale). (c) = Discontinuous and strongly welded quartz mobilisates in a metasedimentary rock directly at the contact to the TGC (marker for scale).

Abb. 8 a-c: Kontakt zwischen Tiger Gabbro Complex und Metasedimentgesteinen des Bower Terranes in einem Kliff an der Nordwestseite von Dragontail Hills (Axt als Maß). (a) = Übersichtsaufnahme des Kontakts (oben: gabbroide Gesteine des Tiger Gabbro Complex; unten: Metasedimentgesteinen des Bowers Terrane; Eisaxt als Maßstab). Die rot gestrichelte Linie markiert den Kontakt. Die gestrichelte Linie endet auf der linken Seite in einer Melange, die zu ca. 90 % aus Schlieren des Nebengesteins besteht, das von einem Netzwerk von gabbroidem Material (ca. 10 %) durchsetzt ist. (b) = Linsen und Schlieren von Nebengesteinen in einem undeformierten Gabbronorit am Kontakt des TGC zu Metasedimentgesteinen des Bowers Terrane (Hammer als Maßstab). (c) = Nicht durchgehende und stark verschweißte Quarzmobilisate in einem Metasedimentgestein direkt am Kontakt zum TGC (Marker als Maßstab).

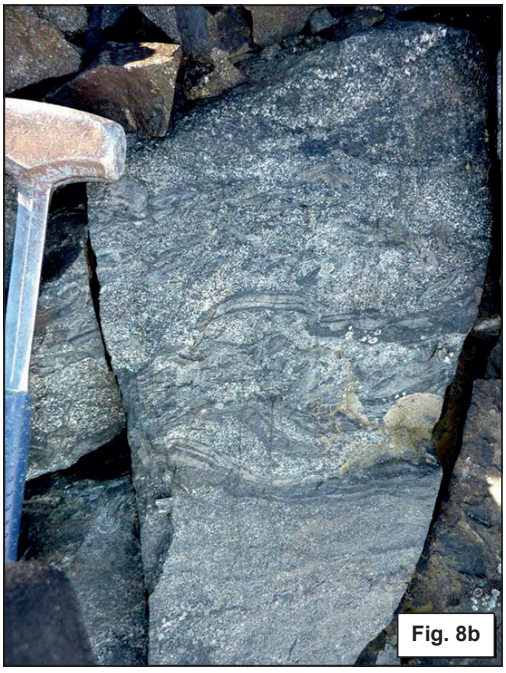

due to plastic flow of the quartz mobilisates induced by very high contact metamorphic conditions. Engel (1987) suggested temperatures close to 800 °C at pressures of 0.2-0.4 GPa in the metasedimentary rocks at the contact. The contact relationships are best explained by a mechanism of forceful intrusion of the still very hot (>>800 °C) TGC into the country rocks at upper crustal levels.

INTERPRETATION AND CONCLUSIONS

Field evidence shows that the TGC is built up by two units: a layered sequence composed of subordinate ultramafic and mainly gabbronoritic to highly evolved anorthositic s.l. cumulate rocks ("layered unit") at Dragontail Hills on the one hand and a massif ultramafic unit showing clear evidence of magma mixing/mingling with gabbroic rocks (similar to the gabbronorite at Dragontail Hills) at Apostrophe Island on the other hand.

Based on our microprobe results, mylonitic gabbroic rocks in the prominent high-temperature shear zones of the TGC at Apostrophe Island record maximum temperature conditions close to the minimum temperature for water-triggered partial melting of gabbroic rocks (c. 870 °C, Beard & Lofgren 1991, Koepke et al. 2004). It is therefore likely that the plagioclase and phenocrystic hornblende-rich melts which synkinematically injected along dominant shear planes were generated by local anatexis during mylonitization. The consistent lineation trend in the shear zones as defined by the elongate hornblende, epidote and chlorite crystals documents that shearing occurred under decreasing temperature conditions. Since later recrystallization processes are not evident and the shear zones show consistent deformational (from mylonitic to

cataclastic) and mineralogical (from high to low-temperature phases) records, we infer that they were formed during the late stage emplacement of the TGC from deeper crustal levels into the Bowers Terrane country rocks at higher-crustal levels and subsequent cooling.

Contact relation between gabbronoritic rocks of the layered unit and country rocks of the TGC at the NW cliff of Dragontail Hills unequivocally demonstrates the intrusive nature of the TGC. Evidence for a tectonic emplacement is missing. Instead, emplacement of the TGC by a mechanism of forceful intrusion at upper crustal levels (ENGEL 1987) seems likely. Bearing in mind that the protoliths of the country rocks, metasedimentary and metavolcanics rocks of the Sledgers Group (Bowers Terrane), have a Middle to Late Cambrian age (summarized in TESSENSOHN & HENJES-KUNST 2005), the age of emplacement of the TGC into the surrounding higher-crustal country rocks must be approximately 490 Ma or younger. This, however, does not exclude that formation of the TGC occurred already earlier in the Cambrian since its cumulate structures are typical for crystallization and accumulation processes occurring in a deeper crustal magma chamber.

We tentatively propose that the TGC records a two-stage evolution during the Ross Orogeny, i.e. an early phase with a maximum age of c. 530 Ma and a late phase with a maximum age of 490 Ma. The first one is related to magmatic processes that were active at deep crustal levels. At that time, the TGC likely crystallized as the lower crustal root zone of the Bowers island arc (BRACCIALI et al. 2009). The latter phase, on the other hand, may be attributed to the late Ross orogenic emplacement of the TGC as a still very hot magmatic complex into the higher-crustal metasedimentary country rocks of the Bowers Terrane under NE–SW directed horizontal maximum stress followed by cooling of the whole complex.

Based on the kinematic data collected from high-temperature shear zones at Apostrophe Island, we suggest that the TGC was deformed by northeast over southwest thrusting. This transport direction is in line with the general NE-SW directed contractional regime reconstructed for the Palaeo-Pacific active continental margin of East Gondwana at that time (e.g., KLEINSCHMIDT & TESSENSOHN 1987). For instance, major thrust zones and cogenetic minor backthrusts in the Wilson Terrane (e.g., Exiles and Wilson thrust system, FLÖTTMANN & KLEINSCHMIDT 1991, LÄUFER et al. 2006, 2011) or at the Bowers Terrane to Robertson Bay Terrane boundary (Millen Thrust Zone, e.g., CRISPINI et al. 2014, PHILLIPS et al. 2014) reveal both southwest and northeast directed reverse tectonic transport and are generally attributed to the late Ross Orogeny.

Further detailed petrological, (isotope) geochemical and geochronological investigations are needed to unravel processes of the magmatic evolution of the TGC. Especially, reliable age data are needed to verify the existing Ar-Ar and Sm-Nd age data and to test the proposed two-stage model. The results so far, however, indicate that the TGC is well suited for evaluating the magmatic and structural evolution of the island-arc type Bowers Terrane at the active continental margin of Palaeo-Victoria Land during the Ross Orogeny and for an in-depth comparison with other examples of exhumed deeper sections of magmatic arc or spreading systems.

ACKNOWLEDGMENT

Franz Tessensohn is sincerely thanked for introducing us into the TGC field relations. Glen Phillips would like to thank the Bundesanstalt für Geowissenschaften und Rohstoffe (BGR) for invitation to GANOVEX X. The fieldwork during the GANOVEX X expedition would not have been possible without the logistic support by the crew of the M/V "Italica" and pilots and mechanics of HELICOPTERS NEW ZEALAND (HNZ). Special thanks are due to the NZ field guide Brian Straite who assisted in the field. This study was supported by the Deutsche Forschungsgemeinschaft (Grant KO 1723/11-1 to J. Koepke) in the framework of the priority program "Antarctic Research with comparative investigations in Arctic ice areas", which is gratefully acknowledged. F. Tessensohn and U. Schüssler are thanked for their careful reviews, which helped to clarify important aspects of the study.

References

Annen, C., Blundy, J.D. & Sparks, R.S.J. (2006): The genesis of intermediate and silicic magmas in deep crustal hot zones.- J. Petrol. 47: 505-539.

Behn, M.D. & Kelemen, P.B. (2006): Stability of arc lower crust: insights from the Talkeetna arc section, south central Alaska, and the seismic structure of modern arcs.- J. Geophys. Res. Solid Earth 111: B11207.

Beard, J.S. & Lofgren, G.E. (1991): Dehydration melting and water-saturated melting of basaltic and andesitic greenstones and amphibolites at 1, 3, and 6.9 kb.- J. Petrol. 32: 365-401.

Bracciali, L., Di Vincenzo, G., Rocchi, S. & Ghezzo, C. (2009): The Tiger Gabbro from northern Victoria Land, Antarctica: the roots of an island arc within the early Palaeozoic margin of Gondwana.- J. Geol. Soc. London 166: 711-724.

Capponi G., Meccheri M. & Oggiano G. (1997): Antarctic Geological 1:250,000 Map series. Coulman Island Quadrangle, (Victoria Land).- Museo Nazionale dell'Antartide, Sezione di Scienze della Terra, Siena, Italy.

Capponi, G., Crispini, L., Di Vincenzo, G., Ghezzo, C., Meccheri, M., Palmeri, R. & Rocchi, S. (2003): Mafic rocks of the Bowers Terrane and along the Wilson-Bowers Terrane boundary: Implications for a geodynamic model of the Ross Orgeny in Northern Victoria Land, Antarctica.- Geophys. Res. Abstr. 5: 05843.

Crispini, L, Federico, L. & Capponi, G. (2014): Structure of the Millen Schist Belt (Antarctica): clues for the tectonics of northern Victoria Land along the paleo-Pacific margin of Gondwana.- Tectonics 33: 420-440, doi:10.1002/2013TC003414.

DeBari, S.M. (1994): Petrogenesis of the Fiabala gabbroic intrusion, northwestern Argentina, a deep-crustal syntectonic pluton in a continental magmatic arc.- J. Petrol. 35: 679-713.

Di Vincenzo, G. & Rocchi, S. (1999): Origin and interaction of mafic and felsic magmas in an evolving late orogenic setting: the Early Paleozoic Terra Nova Intrusive Complex, Antarctica.- Contrib. Mineral. Petrol. 137: 15-35.

Engel, S. (1987): Contact metamorphism by the layered gabbro at Spatulate Ridge and Apostrophe Island (North Victoria Land, Antarctica).- Geol. Jb. B 66: 275-301.

Ernst, W.G. & Liu, J. (1998): Experimental phase-equilibrium study of Al- and Ti-contents of calcic amphibole in MORB – a semiquantitative thermobarometer.- Amer. Mineral. 83: 952-969.

Estrada, S. & Jordan, H. (2003): Early Paleozoic island arc volcanism in the Bowers terrane of northern Victoria Land, Antarctica.- Geol. Jb. B95: 183-207.

Federico, L., Capponi, G. & Crispini, L. (2006): The Ross Orogeny of the transantarctic mountains: a northern Victoria Land perspective.- Int. J. Earth Sci. 95: 759-770.

Flöttmann, T. & Kleinschmidt, G. (1991): Opposite thrust systems in northern Victoria Land, Antarctica: Imprints of Gondwana's Paleozoic accretion.- Geology 19: 45-47.

Ganovex Team (1987): Geological map of North Victoria Land, Antarctica, 1 : 500 000, explanatory notes.- Geol. Jb. B66: 7-79.

Giacomini, F., Tiepolo, M., Dallai, L. & Ghezzo, C. (2007): On the onset and evolution of the Ross Orogeny magmatism in North Victoria Land, Antarctica.- Chem. Geol. 240: 103-128.

Henjes-Kunst, F. & Schüssler, U. (2003): Metasedimentary units of the Cambro-Ordovician Ross Orogen in northern Victoria Land and Oates Land: Implications for their provenance and geotectonic setting from

loc[a]	phase[b]	no.[c]	SiO_2	TiO_2	Al_2O_3	Cr_2O_3	FeO	MnO	MgO	CaO	Na_2O	K_2O	F	Cl	Total	Mg#[d]	An[e]
UV4307 (plagioklase hornblendite)																	
Al	amph	5	44.44	1.09	12.18	n.a.	12.00	0.20	13.80	11.33	1.99	0.18	3.47	0.02	100.69	67.22	
			0.63	*0.10*	*0.60*		*0.37*	*0.02*	*0.59*	*0.22*	*0.16*	*0.03*	*1.62*	*0.01*			
	plag	10	46.43	-	33.88	-	0.14	-	-	17.56	1.62	-	n.a.	n.a.	99.64		85.67
			0.58		*0.55*		*0.06*			*0.60*	*0.29*						
UV4308 (layered gabbro)																	
Al	amph	6	42.72	3.65	12.69	n.a.	11.28	0.12	12.66	11.62	2.64	0.25	-	-	97.64	66.67	
			0.46	*0.18*	*0.19*		*0.24*	*0.02*	*0.23*	*0.15*	*0.10*	*0.02*					
	plag	9	53.07	-	29.56	-	-	-	-	12.34	4.63	0.05	n.a.	n.a.	99.65		59.53
			0.77		*0.34*					*0.59*	*0.26*	*0.03*					
	opx	10	52.76	0.34	2.51	-	18.85	0.39	24.90	0.94	-	-	n.a.	n.a.	100.71	70.19	
			0.49	*0.31*	*0.38*		*0.72*	*0.06*	*0.64*	*0.85*							
	cpx	10	50.72	1.02	4.66	-	7.85	0.18	13.26	21.92	0.69	-	n.a.	n.a.	100.31	75.07	
			0.42	*0.07*	*0.25*		*0.53*	*0.03*	*0.37*	*0.84*	*0.05*						
UV4309 (microgabbronorite)																	
Al	amph	20	41.19	3.50	14.32	n.a.	10.15	0.10	13.35	11.49	2.96	0.78	0.47	-	98.30	70.11	
			0.36	*0.26*	*0.35*		*0.43*	*0.02*	*0.53*	*0.19*	*0.14*	*0.10*	*0.79*				
	plag	21	52.66	-	29.98	-	-	-	-	12.67	4.42	0.13	n.a.	n.a.	99.87		60.80
			0.64		*0.48*					*0.52*	*0.30*	*0.02*					
	opx	14	53.16	0.30	3.16	-	15.94	0.32	26.82	1.09	-	-	n.a.	n.a.	100.78	75.00	
			0.21	*0.06*	*0.32*		*0.36*	*0.04*	*0.32*	*0.50*							
	cpx	13	50.29	1.10	5.06	-	6.91	0.18	14.34	21.50	0.75	-	n.a.	n.a.	100.12	78.73	
			0.34	*0.12*	*0.20*		*0.35*	*0.05*	*0.38*	*0.53*	*0.09*						
	ol	15	38.02	-	-	-	26.05	0.34	36.59	-	-	-	n.a.	n.a.	101.00	71.47	
			0.21				*0.36*	*0.05*	*0.46*								
UV4314 (layered gabbro)																	
Al	amph	15	43.47	2.34	12.38	n.a.	10.30	0.10	14.43	11.86	2.28	0.24	-	0.03	97.43	71.41	
			0.30	*0.04*	*0.25*		*0.47*	*0.02*	*0.25*	*0.17*	*0.06*	*0.02*		*0.00*			
	plag	8	47.91	-	33.19	-	-	-	-	16.52	2.31	-	n.a.	n.a.	99.93		79.84
			0.07		*0.05*					*0.08*	*0.05*						
	opx	15	53.24	0.17	2.70	-	16.97	0.33	26.52	0.67	-	-	n.a.	n.a.	100.60	73.59	
			0.25	*0.04*	*0.62*		*0.75*	*0.04*	*0.73*	*0.19*							
	cpx	8	51.81	0.47	3.30	-	7.08	0.18	14.66	22.43	0.47	-	n.a.	n.a.	100.38	78.68	
			0.07	*0.04*	*0.05*		*0.15*	*0.08*	*0.06*	*0.08*	*0.05*						
UV4316 (hornblende pyroxenite)																	
Al	amph	10	43.40	2.18	12.20	n.a.	9.72	0.08	14.54	12.14	2.59	0.08	-	-	96.93	72.74	
			0.67	*0.21*	*0.43*		*0.41*	*0.02*	*0.49*	*0.18*	*0.10*	*0.03*					
	opx	17	53.74	0.17	2.80	-	14.86	0.27	27.47	0.92	-	-	n.a.	n.a.	100.23	76.73	
			0.45	*0.03*	*0.37*		*0.61*	*0.04*	*0.68*	*0.80*							
	cpx	13	50.33	0.72	4.95	0.18	6.48	-	13.82	22.65	0.54	-	n.a.	n.a.	99.66	79.16	
			0.31	*0.07*	*0.36*	*0.05*	*0.21*		*0.18*	*0.30*	*0.09*						
UV4393 (ferrogabbronorite)																	
Al	amph	8	42.81	3.11	12.37	n.a.	10.48	0.11	13.51	11.64	2.47	0.33	-	0.04	96.86	69.68	
			0.57	*0.27*	*0.51*		*0.28*	*0.03*	*0.36*	*0.20*	*0.10*	*0.06*		*0.01*			
	plag	9	49.01	-	31.89	-	0.18	-	-	15.35	2.90	0.03	n.a.	n.a.	99.36		74.43
			0.77		*0.48*		*0.05*			*0.63*	*0.34*	*0.00*					
	opx	27	53.03	0.21	3.24	-	16.26	0.30	25.32	0.78	-	-	n.a.	n.a.	99.15	73.52	
			0.33	*0.05*	*0.35*		*0.55*	*0.04*	*0.55*	*0.46*							
	cpx	12	50.07	0.78	4.70	0.16	6.66	0.17	13.44	22.57	0.58	-	n.a.	n.a.	99.13	78.24	
			0.89	*0.26*	*0.69*	*0.05*	*0.35*	*0.05*	*0.36*	*0.40*	*0.06*						
FT1435 (amphibole-bearing pyroxenite)																	
Al	amph	9	43.89	2.03	13.31	n.a.	7.32	-	15.78	11.91	2.48	0.23	-	0.03	96.98	79.36	
			0.73	*0.19*	*0.45*		*0.25*		*0.33*	*0.15*	*0.13*	*0.11*		*0.00*			
	opx	10	54.26	0.14	2.78	-	12.22	0.24	29.79	0.62	-	-	n.a.	n.a.	100.05	81.29	
			0.62	*0.03*	*0.25*		*0.29*	*0.06*	*0.24*	*0.20*							
	cpx	8	51.39	0.50	4.14	0.18	5.03	-	14.97	22.44	0.58	-	n.a.	n.a.	99.23	84.13	
			0.22	*0.06*	*0.32*	*0.03*	*0.20*		*0.31*	*0.46*	*0.06*						
FT1436 (porphyroclastic layered gabbro)																	
Al	amph	5	42.99	1.71	13.58	n.a.	8.37	0.09	14.83	12.22	3.04	0.12	-	0.02	96.96	75.96	
			0.45	*0.16*	*0.20*		*0.36*	*0.02*	*0.42*	*0.24*	*0.05*	*0.01*		*0.00*			
	plag	13	47.88	-	32.81	-	0.16	-	-	16.59	2.35	-	n.a.	n.a.	99.79		79.58
			1.05		*0.59*		*0.19*			*0.75*	*0.49*						
	cpx	6	51.19	0.57	4.47	0.24	5.78	0.14	13.44	22.97	0.59	-	n.a.	n.a.	99.39	80.57	
			0.67	*0.13*	*0.96*	*0.07*	*0.25*	*0.04*	*0.29*	*0.94*	*0.24*						
	ol	20	38.80	-	-	-	21.52	0.27	37.93	-	-	-	n.a.	n.a.	98.52	75.86	
			0.26				*0.34*	*0.04*	*0.72*								
	ilm	1	-	52.86	-	-	43.57	1.15	2.13	-	-	-	n.a.	n.a.	99.72	8.03	

Table 1 continued ▶

loc[a]	phase[b]	no.[c]	SiO_2	TiO_2	Al_2O_3	Cr_2O_3	FeO	MnO	MgO	CaO	Na_2O	K_2O	F	Cl	Total	Mg#[d]	An[e]
UV4341 (ferrogabbronorite)																	
DH	amph	10	41.87	2.21	10.60	n.a.	18.08	0.17	9.89	11.03	1.70	1.60	-	0.57	97.73	49.38	
			0.46	*0.14*	*0.31*		*0.35*	*0.02*	*0.38*	*0.17*	*0.07*	*0.09*		*0.05*			
	plag	10	56.23	-	27.40	-	0.16	-	-	9.76	6.72	0.59	n.a.	n.a.	100.84		43.15
			0.62		*0.39*		*0.03*			*0.36*	*0.30*	*0.03*					
	opx	20	50.71	0.16	1.25	-	28.12	0.55	18.67	0.77	-	-	n.a.	n.a.	100.23	54.21	
			0.41	*0.04*	*0.12*		*0.36*	*0.06*	*0.34*	*0.11*							
	cpx	6	51.55	0.40	2.42	-	12.44	0.28	11.77	21.08	0.50	-	n.a.	n.a.	100.44	62.79	
			0.58	*0.10*	*0.33*		*0.70*	*0.05*	*0.32*	*0.52*	*0.05*						
	ilm	9	-	49.88	-	-	49.13	0.60	0.23	-	-	-	n.a.	n.a.	99.84	0.84	
				0.80			*0.64*	*0.05*	*0.04*								
UV4321 (olivine gabbronorite)																	
DH	amph	9	40.76	3.50	14.27	n.a.	10.55	0.11	13.18	11.39	3.24	0.82	-	0.02	97.87	69.01	
			0.36	*0.08*	*0.32*		*0.18*	*0.03*	*0.29*	*0.15*	*0.08*	*0.05*		*0.00*			
	plag	9	50.22	-	31.49	-	0.18	-	-	14.43	3.94	0.12	n.a.	n.a.	100.38		66.50
			0.28		*0.16*		*0.06*			*0.16*	*0.12*	*0.01*					
	opx	10	53.10	0.46	2.74	0.12	15.98	0.32	26.05	1.37	-	-	n.a.	n.a.	100.15	74.40	
			0.31	*0.23*	*0.14*	*0.04*	*0.30*	*0.04*	*0.32*	*0.41*							
	cpx	8	49.79	1.08	4.78	0.19	7.89	0.20	14.04	20.59	0.74	-	n.a.	n.a.	99.30	76.04	
			0.26	*0.05*	*0.24*	*0.03*	*0.78*	*0.04*	*0.65*	*1.21*	*0.04*						
	ol	7	37.66	-	-	-	26.33	0.36	35.76	-	-	-	n.a.	n.a.	100.11	70.77	
			0.13				*0.39*	*0.03*	*0.28*								
UV4324 (anorthosite)																	
DH	amph	10	42.59	1.68	13.10	n.a.	11.38	0.25	13.79	11.44	1.51	0.80	0.26	0.16	96.98	68.35	
			0.42	*0.20*	*0.32*		*0.86*	*0.02*	*0.38*	*0.20*	*0.12*	*0.04*	*0.02*	*0.00*			
	plag	11	51.13	-	30.22	-	0.29	-	-	13.66	3.80	0.15	n.a.	n.a.	99.25		65.97
			0.74		*0.51*		*0.04*			*0.66*	*0.37*	*0.03*					
	mt	6	-	-	-	0.20	92.83	-	-	-	-	-	n.a.	n.a.	93.04		
						0.03	*0.29*										
UV4327 (gabbronorite)																	
DH	amph	10	42.50	2.87	12.63	n.a.	11.39	0.13	13.31	11.61	1.85	0.45	-	0.04	96.79	67.58	
			0.50	*0.18*	*0.26*		*0.13*	*0.03*	*0.36*	*0.18*	*0.17*	*0.02*		*0.00*			
	plag	10	48.20	-	32.66	-	0.23	-	-	15.79	3.00	0.06	n.a.	n.a.	99.93		74.19
			0.22		*0.08*		*0.08*			*0.13*	*0.08*	*0.01*					
	opx	20	52.97	0.22	2.65	-	17.27	0.36	25.99	0.99	-	-	n.a.	n.a.	100.44	72.85	
			0.20	*0.03*	*0.12*		*0.44*	*0.06*	*0.38*	*0.63*							
	cpx	10	51.17	0.72	3.62	-	7.33	0.18	13.90	22.58	0.43	-	n.a.	n.a.	99.93	77.17	
			0.40	*0.09*	*0.51*		*0.12*	*0.06*	*0.27*	*0.48*	*0.06*						
UV4333 (layered gabbronorite)																	
DH	amph	10	43.27	2.87	12.03	n.a.	10.37	0.08	14.66	11.48	2.34	0.46	-	0.01	97.58	71.61	
			0.38	*0.13*	*0.30*		*0.53*	*0.02*	*0.23*	*0.14*	*0.10*	*0.02*		*0.00*			
	plag	10	48.56	-	32.04	-	0.26	-	-	15.60	3.22	0.06	n.a.	n.a.	99.74		72.57
			0.24		*0.19*		*0.04*			*0.16*	*0.08*	*0.01*					
	opx	10	53.65	0.25	2.69	-	15.48	0.29	26.15	0.87	-	-	n.a.	n.a.	99.37	75.07	
			0.13	*0.02*	*0.13*		*0.15*	*0.05*	*0.28*	*0.32*							
	cpx	16	50.32	0.89	4.47	-	6.95	0.17	14.25	21.95	0.61	-	n.a.	n.a.	99.60	78.52	
			0.29	*0.06*	*0.19*		*0.60*	*0.05*	*0.57*	*0.97*	*0.08*						
UV4335 (gabbronorite)																	
DH	amph	16	40.85	3.50	13.55	n.a.	11.65	0.13	13.06	11.32	3.27	0.38	-	0.02	97.73	66.66	
			0.27	*0.51*	*0.20*		*0.27*	*0.02*	*0.40*	*0.26*	*0.11*	*0.02*		*0.00*			
	plag	21	48.66	-	32.46	-	0.22	-	-	15.72	3.15	0.05	n.a.	n.a.	100.26		73.18
			0.66		*0.46*		*0.05*			*0.59*	*0.36*	*0.01*					
	opx	21	52.30	0.40	3.29	-	17.01	0.34	25.42	1.43	-	-	n.a.	n.a.	100.19	72.70	
			0.33	*0.24*	*0.29*		*0.38*	*0.05*	*0.42*	*0.57*							
	cpx	16	49.70	0.95	4.67	-	8.12	0.22	13.99	21.20	0.69	-	n.a.	n.a.	99.54	75.45	
			0.85	*0.10*	*0.38*		*0.53*	*0.04*	*0.65*	*0.81*	*0.04*						
	ilm	8	0.35	49.00	-	0.19	46.09	3.81	0.07	0.31	-	-	n.a.	n.a.	99.84	0.28	
			1.00	*0.54*		*0.05*	*0.95*	*0.26*	*0.03*	*0.78*							
UV4342 (ferrogabbronorite)																	
DH	amph	8	42.58	1.72	12.12	n.a.	13.95	0.11	12.16	11.76	1.17	1.59	0.01	0.29	97.48	60.85	
			0.31	*0.03*	*0.15*		*0.18*	*0.02*	*0.25*	*0.13*	*0.10*	*0.04*	*0.00*	*0.01*			
	plag	10	56.67	-	26.79	-	0.26	-	-	9.39	6.86	0.58	n.a.	n.a.	100.55		41.71
			0.46		*0.36*		*0.07*			*0.42*	*0.23*	*0.02*					
	opx	9	51.39	0.18	1.52	-	25.95	0.52	19.41	1.01	-	-	n.a.	n.a.	99.99	57.15	
			0.31	*0.03*	*0.15*		*0.72*	*0.08*	*0.31*	*0.82*							
	cpx	9	51.02	0.34	2.37	-	11.30	0.25	12.47	21.39	0.52	-	n.a.	n.a.	99.67	66.31	
			0.21	*0.04*	*0.11*		*0.44*	*0.04*	*0.19*	*0.28*	*0.02*						
	ilm	8	-	49.88	-	-	49.81	0.79	0.08	-	-	-	n.a.	n.a.	100.56	0.28	
				0.52			*0.43*	*0.08*	*0.03*								

Table 1 continued ▶

loc[a]	phase[b]	no.[c]	SiO_2	TiO_2	Al_2O_3	Cr_2O_3	FeO	MnO	MgO	CaO	Na_2O	K_2O	F	Cl	Total	Mg#[d]	An[e]
UV4343 (gabbronorite)																	
DH	amph	10	43.78	1.20	9.76	n.a.	15.94	0.16	11.91	11.46	1.62	1.26	0.54	0.36	98.00	57.13	
			0.50	*0.28*	*0.66*		*0.65*	*0.02*	*0.59*	*0.14*	*0.59*	*0.11*	*0.77*	*0.06*			
	plag	10	57.36	-	26.91	-	0.20	-	-	9.19	6.27	0.49	n.a.	n.a.	100.42		43.52
			0.29		*0.13*		*0.05*			*0.15*	*0.17*	*0.09*					
	opx	10	51.64	0.55	1.64	-	25.12	0.51	19.65	1.33	-	-	n.a.	n.a.	100.43	58.24	
			0.74	*0.86*	*0.12*		*0.79*	*0.07*	*0.34*	*0.51*							
	cpx	10	51.26	0.40	2.32	-	11.63	0.31	12.55	20.88	0.52	-	n.a.	n.a.	99.86	65.80	
			0.39	*0.08*	*0.29*		*0.62*	*0.06*	*0.36*	*0.70*	*0.07*						
	ilm	4	-	45.63	-	-	52.65	0.67	-	-	-	-	n.a.	n.a.	98.96		
				0.50			*0.31*	*0.04*									
UV4355 (gabbronorite)																	
DH	amph	10	42.15	3.50	12.56	n.a.	13.85	0.17	11.86	11.15	1.89	0.47	-	0.04	97.65	60.43	
			0.37	*0.66*	*0.37*		*0.16*	*0.03*	*0.11*	*0.15*	*0.08*	*0.04*		*0.01*			
	plag	10	53.04	-	29.69	-	-	-	-	12.71	4.50	0.10	n.a.	n.a.	100.04		60.60
			0.39		*0.18*					*0.27*	*0.14*	*0.01*					
	opx	9	52.11	0.18	2.24	-	21.32	0.42	22.21	1.30	-	-	n.a.	n.a.	99.79	65.00	
			0.50	*0.03*	*0.15*		*0.57*	*0.03*	*0.76*	*0.79*							
	ilm	5	0.08	49.98	0.06	-	47.43	2.57	0.08	-	-	-	n.a.	n.a.	100.19	0.30	
			0.13	*0.53*	*0.07*		*0.64*	*0.07*	*0.11*								
UV4362 (hornblende diorite)																	
DH	plag	4	66.64	-	21.26	-	-	-	-	2.07	11.00	-	n.a.	n.a.	100.98		9.43
			0.37		*0.69*					*0.35*	*0.12*						
UV4363 (hornblende diorite)																	
DH	amph	8	41.12	3.83	12.35	n.a.	15.11	0.24	11.37	10.62	2.55	0.41	0.25	0.04	97.87	57.29	
			0.32	*0.21*	*0.14*		*0.32*	*0.03*	*0.22*	*0.05*	*0.05*	*0.01*	*0.01*	*0.01*			
	plag	6	52.01	-	30.13	-	0.16	-	-	13.19	4.18	0.07	n.a.	n.a.	99.73		63.57
			0.61		*0.49*		*0.05*			*0.53*	*0.29*	*0.03*					
	opx	6	52.23	0.29	2.53	-	20.21	0.47	23.03	1.12	-	-	n.a.	n.a.	99.88	67.01	
			0.26	*0.08*	*0.23*		*0.68*	*0.07*	*0.50*	*0.62*							
	cpx	5	50.35	0.91	3.86	-	9.07	0.24	13.62	21.86	0.50	-	n.a.	n.a.	100.42	72.80	
			0.53	*0.07*	*0.28*		*0.92*	*0.06*	*0.71*	*0.08*	*0.04*						
	ilm	7	-	49.93	-	-	50.16	1.52	-	-	-	-	n.a.	n.a.	101.61		
				0.52			*0.40*	*0.08*									
	mt	6	-	0.09	0.19	-	93.12	-	-	-	-	-	n.a.	n.a.	93.41		
				0.09	*0.14*		*0.75*										
FT1476 (ferrogabbronorite)																	
DH	amph	16	43.12	1.74	10.57	n.a.	16.97	0.15	10.27	11.34	1.17	1.54	-	0.29	97.16	51.89	
			0.70	*0.37*	*0.45*		*0.26*	*0.03*	*0.18*	*0.19*	*0.27*	*0.10*		*0.11*			
	bio	21	37.76	4.13	14.87	n.a.	12.16	-	15.44	-	0.08	9.60	-	0.12	94.16	69.36	
			0.44	*0.25*	*0.34*		*1.18*		*0.64*		*0.04*	*0.26*		*0.01*			
	plag	17	57.66	-	26.26	-	0.19	-	-	8.84	6.20	0.69	n.a.	n.a.	99.83		42.35
			0.44		*0.22*		*0.04*			*0.24*	*0.19*	*0.08*					
	opx	20	51.19	0.13	1.17	-	28.02	0.55	17.08	1.12	-	-	n.a.	n.a.	99.28	52.07	
			0.21	*0.04*	*0.12*		*0.89*	*0.06*	*0.32*	*0.88*							
	cpx	14	51.21	0.38	2.37	-	12.13	0.29	11.23	21.21	0.50	-	n.a.	n.a.	99.32	62.26	
			0.38	*0.06*	*0.36*		*0.77*	*0.04*	*0.28*	*0.86*	*0.06*						
	ilm	12	-	48.25	-	-	50.41	0.48	0.23	-	-	-	n.a.	n.a.	99.36	0.80	
				0.85			*0.87*	*0.07*	*0.19*								

Tab. 1: Compositions of minerals from gabbroic rocks of the Tiger Gabbro Complex.
loc[a] = locality: AI = Apostrophe Island; DH = Dragontail Hills; **phase[b]**: amph = amphibole; cpx = clinopyroxene; ilm = ilmenite; mt = magnetite; ol = olivine; opx = orthopyroxene; pl = plagioclase; bi = biotite; **no.[c]** = number of analyses; **Mg#[d]** = MgO/(MgO + FeO^{tot})•100, molar; **An[e]** = An content of the plagioclase (mol %); **-** = below limit of detection; **n.a.** = not analyzed; **FeO** = FeO^{tot}; **italics** = one standard deviation

Tab. 1: Mineralzusammensetzung von gabbroiden Gesteinen des Tiger Gabbro Complex.
loc[a] = Probenlokalität: AI = Apostrophe Island, DH = Dragontail Hills (Spetulate Ridge); **phase[b]**: amph = Amphibol, cpx = Klinopyroxen, ilm = Ilmenit, mt = Magnetit, ol = Olivin, opx = Orthopyroxen, pl = Plagioklas, bi = Biotit; **no.[c]** = Anzahl der Analysen; **Mg#[d]** = molares MgO/(MgO + FeO^{tot})•100; **An[e]** = An-Gehalt von Plagioklas (in mol %); **-** = unterhalb der Nachweisgrenze; **n.a.** = nicht analysiert; **FeO** = FeO^{tot}; **kursiv** = einfache Standardabweichung.

geochemical and Nd-Sr isotope data.- Terra Antartica 10(3): 105-128.

Henjes-Kunst, F. (2003): Single-crystal Ar-Ar laser dating of detrital micas from metasedimentary rocks of the Ross orogenic belt at the Pacific margin of the Transantarctic Mountains, Antarctica.- In: D.K. FÜTTERER (ed), Antarctic Contributions to Global Earth Sciences. - 9th Int. Symp. Ant. Earth Sci., Terra Nostra 2003/4: 150-151.

Holland, T.J.B. & Blundy, J. (1994): Non-ideal Interactions in calcic amphiboles and their bearing on amphibole plagioclase thermometry.- Contrib. Mineral. Petrol. 116: 433-447.

Jagoutz, O., Muntener, O., Ulmer, P., Pettke, T., Burg, J.P., Dawood, H. & Hussain, S. (2007): Petrology and mineral chemistry of lower crustal intrusions: the Chilas Complex, Kohistan (NW Pakistan).- J. Petrol. 48: 1895-1953.

Kleinschmidt, G. & Tessensohn, F. (1987): Early Paleozoic westward directed subduction at the Pacific margin of Antarctica.- In: G. MCKENZIE (ed): Gondwana Six: Structure, Tectonics and Geophysics, Amer. Geophys. Union AGU, Washington D.C., Geophys. Monogr. 40: 89-105.

Kreuzer, H., Höhndorf, A., Lenz, H., Müller, P. & Vetter, U. (1987): Radiometric ages of pre-Mesozoic rocks from northern Victoria Land, Antarctica. In: G. MCKENZIE (ed): Gondwana Six: Structure, Tectonics, and Geophysics, Amer. Geophys. Union AGU, Washington D.C., Geophys. Monogr. 40: 31-47.

Koepke, J., Berndt, J. & Bussy, F. (2003): An experimental study on the shallow-level migmatization of ferrogabbros from the Fuerteventura Basal Complex, Canary Islands.- Lithos 69: 105-125.

Koepke, J., Feig, S.T., Snow, J. & Freise, M. (2004): Petrogenesis of oceanic plagiogranites by partial melting of gabbros: An experimental study.- Contrib. Mineral. Petrol. 146: 414-432.

Koepke, J., France, L., Müller, T., Faure, F., Goetze, N., Dziony, W. & Ildefonse, B. (2011): Gabbros from IODP Site 1256 (Equatorial Pacific): Insight into axial magma chamber processes at fast-spreading ocean ridges.- Geochem. Geophys. Geosyst. 12: doi:10.1029/2011GC003655.

Läufer, A.L., Kleinschmidt, G. & Rossetti, F. (2006): Late-Ross structures in the Wilson Terrane in the Rennick Glacier area (northern Victoria Land, Antarctica).- In: D.K. FÜTTERER, D. DAMASKE, G. KLEINSCHMIDT, H. MILLER & F. TESSENSOHN (eds), Antarctica: Contributions to Global Earth Sciences, Springer-Verlag, Berlin Heidelberg New York: 195-204.

Läufer, A.L., Lisker, F. & Phillips, G. (2011): Late Ross-orogenic deformation of basement rocks in the northern Deep Freeze Range, Victoria Land, Antarctica: the Lichen Hills Shear Zone.- Polarforschung 80(2): 60-70.

McDougall, I. & Harrison, T.M. (2000): Geochronology and thermochronology by the $^{40}Ar/^{39}Ar$ method.- Oxford Univ. Press, New York, 2nd Edition, 1-269.

Passchier, C.W. & Trouw, R.A.J. (2005): Microtectonics.- Springer-Verlag, Berlin Heidelberg New York, 2nd Edition: 1-366.

Phillips, G., Läufer, A. & Piepjohn, K. (2014): Geology of the Millen Thrust System, northern Victoria Land, Antarctica.- Polarforschung 84: 39–47 (this volume)

Ricci, C.A. & Tessensohn, F. (2003): The Lanterman–Mariner suture: Antarctic evidence for active margin tectonics in Paleozoic Gondwana.- Geol. Jb. B85: 303-332.

Rocchi, S., Di Vincenzo, G., Tonarini, S. & Ghezzo, C. (1999): The Tiger Gabbro of northern Victoria Land: Age, affinity and tectonic implications.- 8th Internat. Sympos. Antarctic Earth Sci. ISAES, Progr. & Abstracts, Wellington, NZ Abstract Volume: 270.

Rocchi, S., Capponi, G., Crispini, L., Di Vincenzo, G., Ghezzo, C., Meccheri, M. & Palmeri, R. (2003): Mafic rocks at the Wilson-Bowers Terrane transition and within the Bowers Terrane: Implications for a geodynamic model of the Ross Orogeny.- Terra Antartica Rep. 9: 145-148.

Tessensohn, F. & Henjes-Kunst, F. (2005): Northern Victoria Land Terranes, Antarctica: far travelled or local products?- In: A.P.M. VAUGHAN, P.T. LEAT & R.J. PANKHURST (eds), Terrane Processes at the Margins of Gondwana, Geol. Soc. London, Spec. Publ. 246: 275-291.

Tiepolo, M. & Tribuzio, R. (2008): Petrology and U-Pb zircon geochronology of amphibole-rich cumulates with sanukitic affinity from Husky Ridge (northern Victoria Land, Antarctica): Insights into the role of amphibole in the petrogenesis of subduction-related magmas.- J. Petrol. 49: 937-970.

Tribuzio, R., Tiepolo, M. & Fiameni, S. (2008): A mafic-ultramafic cumulate sequence derived from boninite-type melts (Niagara Icefalls, northern Victoria Land, Antarctica).- Contrib. Mineral. Petrol. 155: 619-633.

Weaver, S.D., Bradshaw, J.D. & Laird, M.G. (1984): Geochemistry of Cambrian volcanics of the Bowers Supergroup and implications for the Early Palaeozoic tectonic evolution of northern Victoria Land, Antarctica.- Earth Planet. Sci. Lett. 68: 128-140.

Winter, J.D. (2001): An introduction to igneous and metamorphic petrology.- Prentice Hall, 1-697.